EX VIVO MICROWAVE ABLATION APPLICATION AT 2.45 GHz BY A NOVEL NITI SHAPE MEMORY ALLOY BASED RING ANTENNA

Ahmet Rifat GÖRGÜN[1*], Adnan KAYA[2], Selçuk ÇÖMLEKÇİ[3]

[1] Isparta Uygulamalı Bilimler Üniversitesi, Teknik Bilimler Meslek Yüksek Okulu, Elektronik Teknolojisi, Isparta, ORCID No : 0000-0003-1416-5570

[2] İzmir Katip Çelebi Üniversitesi, Mühendislik ve Mimarlık Fakültesi, Elektrik ve Elektronik Mühendisliği Bölümü, İzmir, ORCID No : 0000-0002-9943-6925

[3] Süleyman Demirel Üniversitesi, Mühendislik Fakültesi, Elektrik Elektronik Mühendisliği Bölümü, Isparta, ORCID No : 0000-0003-1389-6435

Keywords

Microwave ablation
Ring antenna
Ex vivo
NiTi (nickel titanium)

Abstract

Although the most preferred treatment methods in cancer treatment are still surgery and chemotherapy, microwave ablation, one of the minimally invasive thermal ablation techniques, is increasingly used in the clinic for patients who cannot afford the risks of these treatment methods. In this study, microwave ablation with a new NiTi ring antenna was performed on a freshly slaughtered beef liver as an Ex Vivo application. Design and optimization was carried out in the CST Microwave studio. Ex Vivo MWA application was carried out at 2.45 GHz, using 50 W microwave power for 5 minutes. The lowest width of the ablation zone formed along the x-axis was 14.58 mm, the highest width was 28.61 mm, the length of the ablation area along the y-axis was 58.032 mm, and the area of the ablation zone was approximately 5.44 cm2. These results show that the proposed NiTi ring antenna has the ability to achieve a sufficient thermal lesion in terms of ablation zone dimensions.

YENİ BİR NİTİ ŞEKİL HAFIZALI ALAŞIM TABANLI HALKA ANTEN İLE 2.45 GHz'DE EX VIVO MİKRODALGA ABLASYON UYGULAMASI

Anahtar Kelimeler

Mikrodalga ablasyon
Halka anten
Ex vivo
NiTi (nikel titanyum)

Öz

Kanser tedavisinde en çok tercih edilen tedavi yöntemleri hala cerrahi ameliyat ve kemoterapi olsa da, bu tedavi yöntemlerindeki riskleri kaldıramayacak hastalarda, minimal invaziv termal ablasyon tekniklerinden biri olan mikrodalga ablasyon uygulaması gittikçe artan bir oranda klinikte kullanılmaktadır. Bu çalışmada, Ex Vivo uygulaması olarak yeni kesilmiş bir sığır karaciğerine yeni bir NiTi halka anten ile mikrodalga ablasyon uygulaması gerçekleştirilmiştir. Tasarım ve optimizasyon CST Mikrodalga stüdyoda gerçekleştirilmiştir. Ex Vivo MWA uygulaması, 2.45 GHz' de, 50 W mikrodalga gücünün 5 dakika süresince kullanılmasıyla gerçekleştirilmiştir. x ekseni boyunca oluşturulan ablasyon bölgesinin en düşük genişliği 14,58 mm, en yüksek genişliği 28,61 mm, y ekseni boyunca elde edilen ablasyon alanının uzunluğu 58.032 mm ve ablasyon bölgesi alanı ise yaklaşık 5.44 cm^2 olarak elde edilmiştir. Elde edilen bu sonuçlar önerilen NiTi halka antenin ablasyon bölgesi boyutları açısından yeterli bir termal lezyonu başarma kabiliyetine sahip olduğunu göstermektedir.

Araştırma Makalesi		Research Article	
Başvuru Tarihi	: 03.08.2022	Submission Date	: 03.08.2022
Kabul Tarihi	: 24.02.2023	Accepted Date	: 24.02.2023

* Sorumlu yazar: agahmetgorgun@gmail.com.tr
https://doi.org/ 10.31796/ogummf.1111038

1. Introduction

Liver cancer is the second most common type of cancer in cancer-related deaths in the world, and surgical treatment methods such as resection and transplantation have become standard among possible treatment methods, especially for early-stage Hepatocellular Carcinoma (HCC). However, it has also been noted that surgical resection is not possible in more than 75% of patients with liver cancer (Liu, Zhang, and Jiang,2003; Torre, Siegel, Ward, and Jemal, 2016). The thermal therapy commonly used to treat hepatic cancer include radiofrequency ablation, cryoablation, and microwave ablation. Radiofrequency ablation has disadvantages such as high impedance between the electrode and the ground plate as a result of the blood vessel making the ablation temperatures too low to completely destroy cancer cells and the increase in tissue temperature during application if the targeted area is adjacent to a high flow blood vessel. In addition, the diameter of the tissue coagulated by the RF electrodes is limited to 1.6 cm. This is because the higher energy to achieve larger coagulation diameters causes charring of the tissue near the electrode. This increases local tissue impedance, reduces RF accumulation, heat diffusion, and coagulation necrosis (Goldberg et al., 1998; Lencioni et al., 1998; Goldberg et al., 1995). Cryoablation (CA), which uses cold compressed argon gas to destroy cancer tissue, has advantages such as minimal damage to large vessels, low incidence of pain and controllable ice sphere formation. However, in addition to these advantages, it also has important disadvantages such as the ablation area being limited to the small areas surrounding the cryoablation needles and the possibility of damaging the phrenic nerve (Liu et al., 2020; Seifert, Junginger, and Morris, 1998; Phasukkit, and Wongketsada, 2021). MWA is a thermal therapy used in the treatment of tumors in various tissue types such as liver, lung, breast, kidney and bone. In this therapy, electromagnetic energy is directed to the tumor for a few minutes with an interstitial antenna, in order, EM power is absorbed by the tumor tissue, and the absorbed power heats the tumor tissue, and when the temperature reaches stotoxic levels, between 60°C and 100°C, coagulation necrosis occurs on the tissue. In antenna design, the lowest possible return loss is desired for maximum energy transfer to the tissue. The frequency used is generally 915 MHz and 2.45 GHz. Since the majority of hepatic tumors such as liver tumors and lung tumors are spherical, it is preferred that the ablation pattern of the antenna to be used is approximately spherical (Mohtashami, Hagness, and Behdad, 2017; Yang et al., 2006; Yang, Converse, Mahvi, and Webster, 2007; Luyen, Hagness, and Behdad, 2017; Liu et al., 2016; Etoz, and Brace, 2018; Ahmed, Brace, Lee, and Goldberg, 2011; Luyen, Hagness, and Behdad, 2015; Hodgson et al., 1999; Prakash, 2010). Therefore, in our study, it was preferred to use an antenna type with an approximately spherical ablation pattern.

MWA has some advantages over other thermal treatment methods. Advantages such as low cost, simultaneous use with multiple applicators, shorter ablation time, larger ablation area due to blood perfusion, lower infection risk, lower recovery time, ability to cause necrosis in deeply located tumors, and very lower cancer recurrence can be counted among these (Wrigh, Lee, and Mahvi, 2003; Andreano, Huang, Meloni, Lee, and Brace, 2010; Wright et al., 2005; Lubner, Brace, Hinshaw, and Lee, 2010; Hancock, 2011; Hassan, Takruri, and Hope, 2016; Hubner et al., 2019; Reimann et al., 2019; Shock et al., 2004). MWA is stronger than other thermal ablation methods in organs with high blood perfusion such as the liver, so it is frequently used in the treatment of liver cancer (Brace,2020). In the literature, various antennas such as slot, monopole, dual slot, multi slot, dipole, choke dipole, triaxial, helical, floating sleeve and loop antennas have been used for microwave heating (Mohtashami, Hagness, and Behdad, 2017; Yang et al., 2006; Luyen, Hagness, and Behdad, 2015; Brace, 2011; Ge et al., 2018; Hurter, Reinbold, and Lorenz, 1991; Mohtashami et al., 2018; Brace, Laeseke, Van der Weide, and Lee, 2005; Sugiyama, Saito, 2018). With its simple geometry, circular loop antennas are preferred in many application areas, especially near field communication and RFID applications. For a circular loop carrying a uniform current, near-field expressions such as simple and precise fields and areas along the loop axis can be generated from full general field expressions as special cases, while far fields for a circular loop antenna on the ground plane can be derived from general field expressions (Hamed et al., 2014). Loop antennas are also used in intracranial pressure monitoring, which provides detailed information about the brain, blood and cerebrospinal fluid (Tamilarasan, Krishnadhas, Sabapathy, and Sarasa, 2021). Loop antennas are classified as circular, rectangular and square in shape, and electrically classified as small antennas and large antennas. While the design time, limited bandwidth, antenna size and difficulties in radiation efficiency are the parts that need to be studied, while it is easy and low cost to construct, simple, and an omnidirectional antenna for many important applications. In addition, it is less affected by environmental noise as it does not need ground plane (Ako et al., 2019; Bolton, 2016). The human body decreases the electric field and increases the magnetic field because its conductivity is low. This led to the idea that electrically small (loop's circumference < 0.3 λ)magnetic loop antennas are the most efficient antennas for wearable miniature equipment such as pagers and RF tags (Niekerk et al., 2002; Fujimoto, and James, 2001).. If the circumference of a loop antenna is smaller than the wavelength, there is a problem of matching the radiation resistance with a 50 ohm transmission line (Balanis, 1982). The SAR pattern is one of the most important parameters for MWA and shows the energy absorbed by the tissue, in other words, the heating ability of the MWA system. In addition, the shape of the ablation zone is also highly dependent on the SAR distribution.

In this study, Ex Vivo MWA application was performed on a freshly cut beef liver using a NiTi shape memory alloy-based ring antenna produced by us and presented in our previous study (Gorgun, Çomlekci, and Kaya, 2019), using 50 W microwave power at 2.45 GHz for 5 minutes, and the relevant results are presented.

2. Method

2.1. SMA (Shape Memory Alloy) Material

NiTi alloys are frequently used in biomedical surgical devices and biomedical applications due to their features such as superior corrosion resistance, biocompatibility, magnetic resonance, computed tomography compatibility, especially with minimally invasive surgery, which is one of the most important advances in the field of modern medicine (Fadlallah, El-Bagoury, Gad, Ahmed, and El-Ousamii, 2014; Morgan, 2004; Holton, Walsh, Anayiotos, Pohost, and Venugopalan, 2002; Song, 2010).

2.2. Method of Antenna Preparation

In the realization of novel and NiTi SMA based ring antenna, coaxial cable is also used together with NiTi SMA wire. The characteristics of this coaxial cable used are presented in Table 1.

Table 1. Coaxial Cable Specifications

	Material	Diameter
Inner Conductor	StCu, Silver plated	0.53 mm
Dielectric	PTFE (polytetrafluorethylene)	1.65 mm
Cable Sheath	Braid + Band copper, tin plated	2.10 mm

The CST drawing of the NiTi ring antenna is presented in Figure 1.

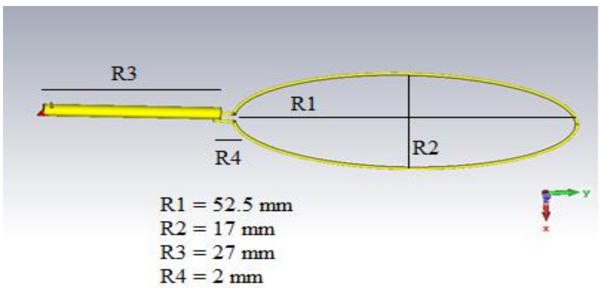

Figure 1. Dimensions and CST Drawing of NiTi Ring Antenna

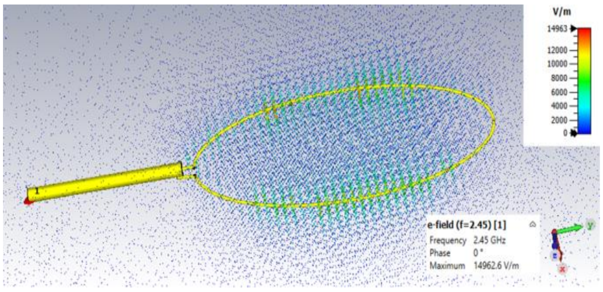

Figure 2. E-Field

As shown in Figure 2, the maximum electric field value 2.45 GHz at 14963 (V / m).

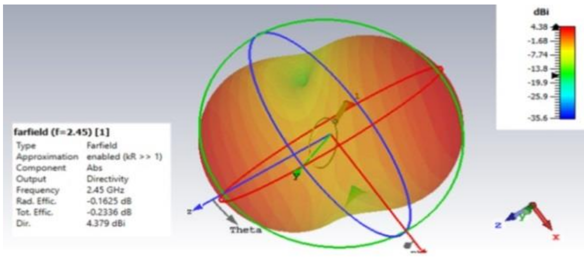

Figure 3. Directivity

As shown in Figure 3, the directivity was 4.38 dBi at 2.45 GHz.

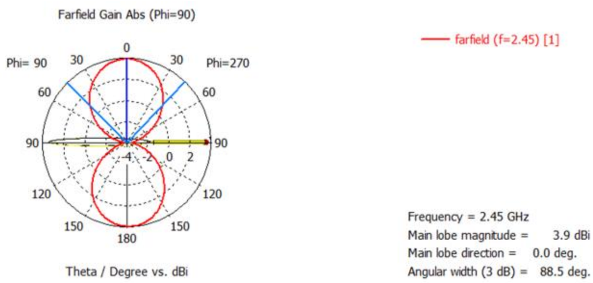

Figure 4. Farfield Gain Abs (Phi=90)

Farfield gain abs (Phi=90) is presented in Figure 4 at 2.45 GHz.

(a)

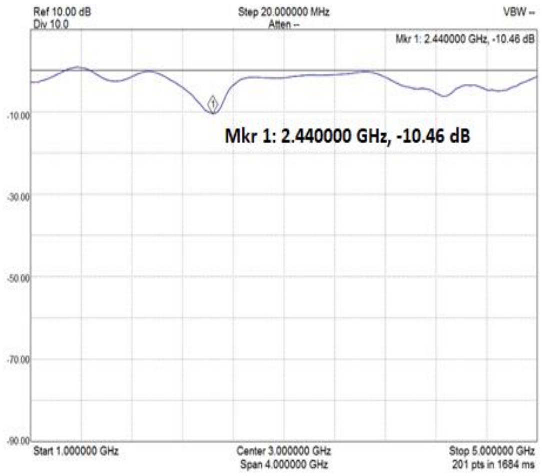

(b)

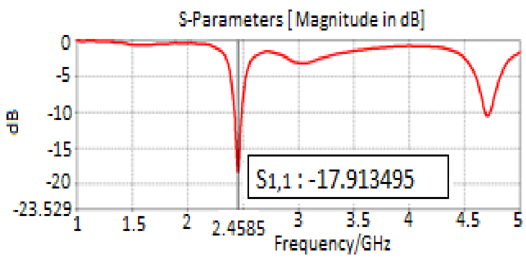

(c)

Figure 5. a) NiTi Ring Antenna b) Return loss (S_{11}) measurement of NiTi ring antenna at 2.44 GHz. c) Return loss (S_{11}) simulation of NiTi ring antenna at 2.45 GHz.

As seen in Figure 5.b, return loss of proposed antenna was measured as -10.46 dB at 2.44 GHz. And as seen in Figure 5.c, return loss of proposed antenna was simulated as -17.91 dB at 2.45 GHz.

Especially since the 0.5 mm diameter NiTi SMA wire added to the end of the coaxial cable is a hard material, it could not be made into a full ellipse as in the simulated image of the antenna. This is the most important reason for the difference between the above simulation and measurement S11 results.

2.3. Circle Shape NiTi Wire Preparation Process

A novel and NiTi SMA-based ring antenna was realized by adding 0.5 mm diameter NiTi wire to the end of the 27 mm long coaxial cable, one end to the inner conductor of the coaxial cable and the other end to the outer conductor, adding an elliptical ring with a diameter of 17 mm and a long diameter of 52.5 mm.

2.4. Mathematical Descriptions of the Simulation Models

The dimensions of the model components are given in Table 2.

Table 1. Dimensions of Model Components

Components	Dimensions	
	Length (mm)	Diameter (mm)
Inner Conductor	27	0.51
Dielectric	27	1.68
Outer conductor	27	2.20
Catheter	27	2.40
Components	Dimensions	
	Diameter of NiTi wire (mm)	Short diameter/ Long diameter of the ellipse (mm)
NiTi Ring Antenna	0.5	17.0/ 52.5

2.5. Temperature Analysis Procedure

The bioheat transfer equation used to obtain the temperature distribution of the living tissue is shown in equation (1).

$$\rho c \frac{\partial T}{\partial t} = k\nabla^2 T - \rho\rho_b c_b F(T - T_b) + Q \quad (1)$$

where ρ is the tissue density $(kg.m^{-3})$, c is the specific heat capacity of the tissue $(J.kg^{-1}.K^{-1})$, T is the temperature, t is the heat transfer time, k is the thermal conductivity $(W.m^{-1}.K^{-1})$, ρ_b is the blood density $(kg.m^{-3})$, c_b is the specific heat capacity of the blood $(J.kg^{-1}.K^{-1})$, F is the blood flow rate $(m^3.kg^{-1}.s^{-1})$, T_b is the temperature of the blood, and Q is the is the energy deposited by the antenna into the tissue $(W.m^{-3})$.

$$\omega_b = \rho F \quad (s^{-1}) \quad (2)$$

where ω_b is the blood perfusion rate, ρ is the tissue density ($kg.m^{-3}$), and F is the blood flow rate ($m^3.kg^{-1}.s^{-1}$).

$$Q = \sigma|E|^2 = \rho SAR = J.E \quad (W.m^{-3}) \tag{3}$$

Where Q is the is the energy deposited by the antenna into the tissue ($W.m^{-3}$), σ is the tissue conductivity ($S.m^{-1}$), ρ is the tissue density ($kg.m^{-3}$), E is the applied electric field ($V.m^{-1}$), SAR is the spesific absorption rate ($W.kg^{-1}$), and J is the current density ($A.m^{-2}$).
Equation 4 is obtained by putting the equations 2 and 3 in their places in the equation 13.

$$\rho c \frac{\partial T}{\partial t} = k\nabla^2 T - \rho_b c_b \omega_b (T - T_b) + \rho SAR \tag{4}$$

In Ex Vivo applications, $\omega_b = 0$ is taken as there is no perfusion.

The initial temperatures of the tissue, blood, and air are all 37 °C. Thermal constants are shown in Table 3.

Table 3. Electromagnetic properties at 2.45 GHz and Thermal Properties of liver Tissue (Kaur, and Maini, 2014; Dielectric Properties of Body Tissues, 2021)

Properties	Value
Thermal conductivity, liver (k) [W/mK]	0.56
Specific heat capacity, blood (c_b) [J/kgK]	3639
Specific heat capacity, liver (c) [J/kgK]	3600
Density, blood (ρ_b) [kg/m^3]	1000
Density, liver (ρ) [kg/m^3]	1020
Blood perfusion rate [$1/s$]	.0036
Blood temperature [$degC$]	37.00
Relative permittivity, liver (ε_r)	43.03
Electric conductivity, liver (σ) [S/m]	1.69
Relative permittivity, dielectric	2.03
Relative permittivity, catheter	2.60

2.6. Microwave Ablation

MWA is a safe minimally invasive treatment method, which is among the thermal therapy methods and applied in cancer treatments. This method is usually performed at ISM frequencies of 915 MHz or 2.45 GHz. In MWA application, the electromagnetic waves produced are directed to the tumor tissue by means of a suitable antenna. As a result of the absorption of the power produced by the electromagnetic wave by the tissue, the polar water molecules in the tissue begin to oscillate rapidly with this magnetic field. For this reason, as a result of the frictional heat generated, the ablation area heats up and cell death occurs when the temperature exceeds 60 degrees, which causes necrosis of tumor cells. The dielectric permeability and conductivity of the tissue are also very important parameters in the absorption of electromagnetic power by the tissue. In particular, the amount of power applied, the specific absorption rate, the rate of blood perfusion, the ablation time, the thermal properties of the environment, the MWA antenna type and diameter used, the size of the ablation zone and the maximum temperature level reached (Seki et al., 1994; Liang, Wang, 2007; O'Rourke et al., 2007; Nan et al., 2013).

The assumption that the targets to be treated are spherical in shape and that there is isotropic energy dissipation can generally be met for tumors smaller than 2.5 cm. Therefore, heating large areas deviates from the ideal ablation model due to the heterogeneous nature of tissue properties over 2.5 cm. It is necessary to pay attention to the optimum ablation time in order to obtain a situation in which MWA application will cause the least damage to the surrounding healthy tissues.

2.7. System Concept

VSGA25 as vector signal generator used. The VSGA25 provided the system with a 2.45 GHz continuous sine wave with 0 dBm output, 1kHz simulation rate and 50% depth. Its 0 dBm output is amplified by a 2.45 GHz, 100W CGHV40100F power amplifier powered by a DC power supply. NiTi Ring antenna is connected to the output of the power amplifier. During the MWA application, the temperature was monitored by Xbee & Arduino-based wireless data transfer using DSD18B20 sensors. The MWA application setup diagram and the pictures of the realized MWA application setup are given in Figure 6.

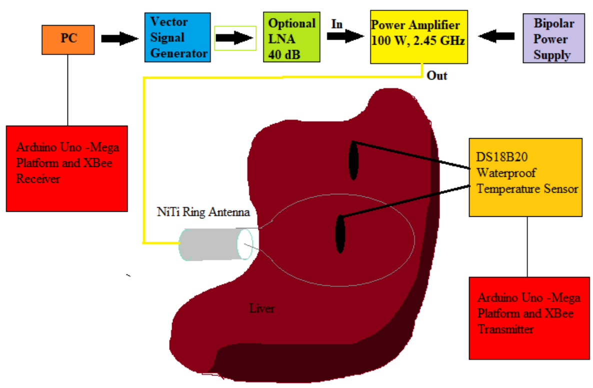

(a)

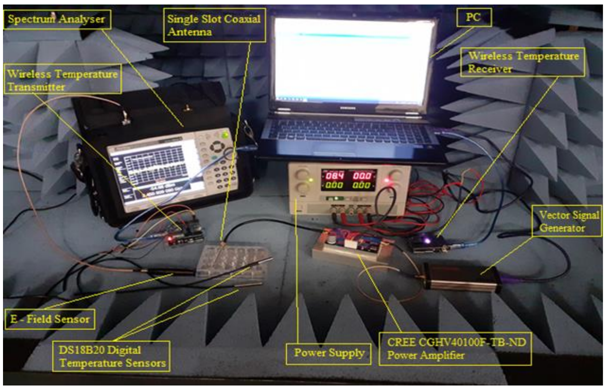

(b)

Figure 6. a)MWA Application Setup Block Diagram b) Realized MWA Application Setup with NiTi Ring Antenna at 2.45 GHz.

In this study, as a power amplifier, the CREE CGHV40100F-TB-ND of Cree is utilized which hosts an unmatched, GaN HEMT. The image of CGHV40100F-ND GaN HEMT power transistor, and the circuit diagram of the power amplifier are given in Figure 6.

3. Results

3.1. MWA Application at 2.45 GHz on Freshly Cut Beef Liver with NiTi Ring Antenna

For different input values at 2.45 GHz, forward power, and reverse power values are given in Table 4.

Table 4. Forward Power, and Reverse Power Values for Different Input Value at 2.45 GHz

Frequency	VGSA Vector Signal Generator (AM modulated sine wave) Amplitude	Forward Power	Reverse Power
2.45 GHz	−20 dBm	32.35 dBm	19.79 dBm
2.45 GHz	−10 dBm	43.37 dBm	27.37 dBm
2.45 GHz	0 dBm	47.92 dBm	35.18 dBm

In Signal Hound VSGA25 100 MHz - 2.5 GHz Vector Signal Generator which will last 100 W, 2.4 GHz - 2.5 GHz PA according to Figure 7, the frequency was set to 2.45 GHz, amplitude was set to 0 dBm and modulation type was set to AM ((Modulation speed: 1 kHz, Modulation depth: 50%, Modulation format: Sine Wave) and driven. The VGS25A Vector Signal Generator in MWA setup was applied to our sine wave antenna with an amplitude of 0 dBm, 47.92 dBm (about 50 W) AM at 2.45 GHz. The relationship between temperature obtained by thermal camera and application time is presented below.

3.2. MWA Implementation Results Performed with NiTi Ring Antenna at 2.45 GHz

Liver images obtained depending on the durations of application are presented in Figure 8.

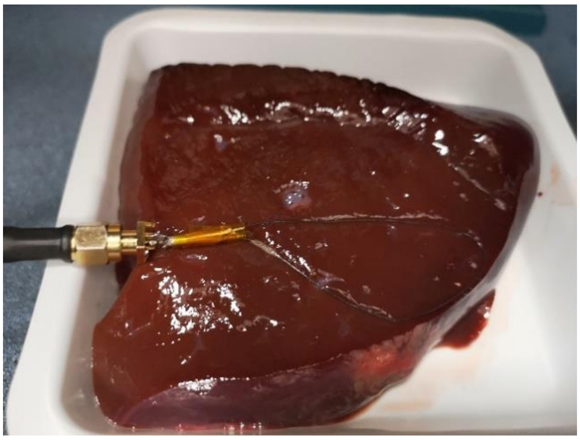

(a)

(b)

(c)

(d)

Figure 7. Liver Images Obtained Depending on the Durations of Application (**t**) in MWA Application Performed, a) $\mathbf{t = 0}$, b) $\mathbf{t = 1\ min}$, c) $\mathbf{t = 3\ min}$, d) $\mathbf{t = 4.5\ min}$

Figure 7. (a) of freshly cut beef liver before MWA application, Figure 7. (b), Figure 7. (c), and Figure 7. (d). MWA application is the 1st min end view, 3rd min end view and the view at the end of 4 and a half minutes, respectively.

(a)

(b)

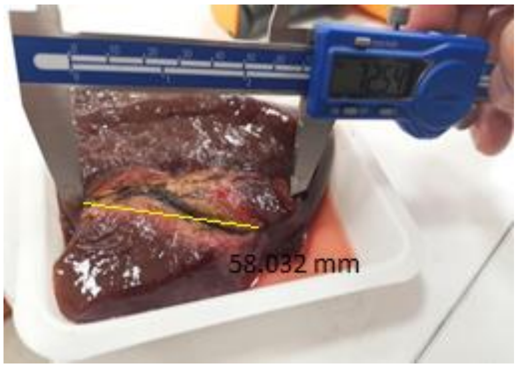

(c)

Figure 8. Dimensions of Ablation, a) Vertical Section Minimum Ablation Zone Size, b) Vertical Section Maximum Ablation Zone Size and c) Horizontal Section Maximum Ablation Zone Size.

At the end of the 5th minute, ablation regions formed in freshly cut beef liver are shown in Figure 8. (a) Figure 8. (b) and Figure 8. (c). As seen in Figure 8. (c), the lowest width of the ablation zone formed along the x axis is 14.58 mm, as seen in Figure 8. (b), the highest width of the ablation zone formed along the x axis is 28.61 mm and As can be seen in Figure 8. (c), the length of the ablation area obtained along the y axis was measured as 58.032 mm after 5 minutes of microwave ablation application with 50 W power.

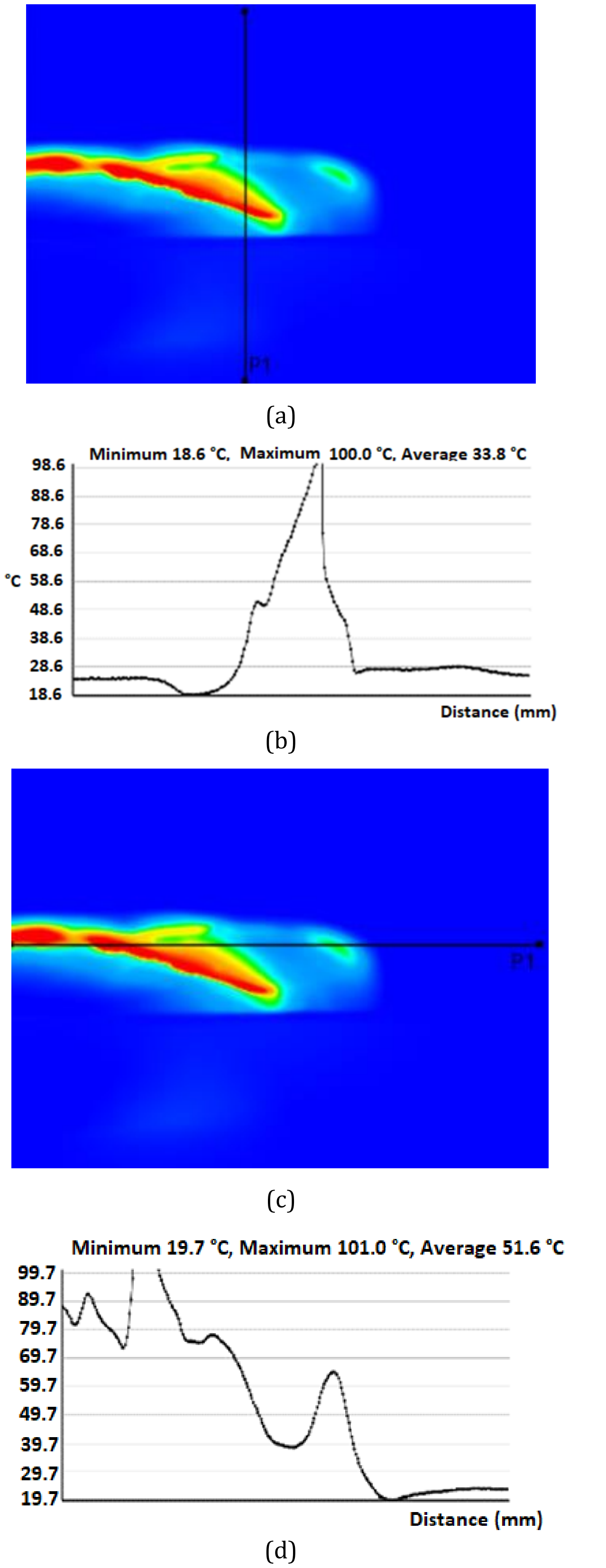

Figure 9. a) Thermal Camera Image Vertical Section Axis, b) Temperature Distance Relationship along the Vertical Axis Line, c) Thermal Camera Image Horizontal Section Axis, d) Temperature Distance Relationship along the Horizontal Axis Line

According to the temperature distance graph obtained along the vertical axis line in Figure 9. (b), it is observed that a minimum of 18, 6 °C, maximum 100 °C in the regions seen in red and average 33.8 °C temperatures are reached.

According to the temperature distance graph obtained along the vertical axis line in Figure 9. (d), it is seen that minimum 18.7 °C, maximum 101 °C in the regions seen in red and average 51.6 °C temperatures are reached.

Looking at the literature, coaxial slot antennas are frequently used in cancer treatments with MWA. Some of the similar studies in the literature (Ibitoye et al., 2015; Yang et al., 2006; Amabile et al., 2017) and our study are presented in Table 5 comparatively. The originality of our study is that it is a ring antenna based on NiTi shape Memory alloy and the resultant approximate ellipsoid ablation area is comparable to the studies in the literature in terms of ablation length, ablation diameter and ablation zone area. It is thought to be a usable antenna, especially in large-scale skin tumors. The comparison of this study with similar studies in the literature is presented in Table 5.

Table 5. The Comparison of This Study with Similar Studies in the Literature

Antenna Type	Input power/ Ablation duration	Ablation length/ Ablation diameter	Ablation zone shape	Ref
Dual slot antenna metallic sleeve antenna	50 W/ 5 Min	44.3± 0.4 mm / 34.4± 0.6 mm	ellipsoid	(Ibitoye et al., 2015)
Floating sleeve antenna	120 W/ 2.5 Min	5.87± 0.32cm / 3.64± 0.33 cm.	ellipsoid	(Yang et al., 2006)
Miniaturized sleeve choke coaxial antenna	60 W / 5 Min	4.8 ± 0.2 cm / 3.4 ± 0.3 cm	ellipsoid	(Amabile et al., 2017)
NiTi ring antenna	50 W/ 5 Min	58.03 ± 0.2 mm / 21.59 ± 0.1 mm	ellipsoid	This work

In terms of the obtained ablation zone diameter and the horizontal and vertical maximum lengths of the ablation zone, results close to the studies in the literature were obtained.

4. Conclusions

MWA applications are generally used as a minimally invasive method in liver and lung tumors as an alternative to treatment options such as chemotherapy and surgical applications, especially in elderly or severe patients who cannot undergo surgery. In liver and lung tumors, which are generally spherical, it is necessary to heat the tumor to 60 centigrade degrees, where coagulation will occur, by heating the tumor with the noninvasive or minimally invasive MWA application in a short period of 3-5 minutes, thus rendering the tumor ineffective. In addition, in order to reduce the invasiveness of all these, it is necessary to apply high Watt to the tumor tissue, to raise the relevant tissue above 60 centigrade in a short time, to perform the MWA application with an antenna with a spherical radiation pattern, since the tumor is spherical, and to obtain a wider ablation area for tumors larger than 2.5 cm. Again, in addition to the high directivity of the antenna, the fact that it is designed from a material with high biocompatibility and corrosion resistance at high temperatures is due to all these requirements.

Designed NiTi ring antenna by adding NiTi wire to the end of the coaxial cable is an MWA antenna that can be used especially in wide cancer region. Computational results were obtained with MWA application in ex vivo bovine liver at 2.45 GHz, by using 50 W microwave power for 5 minutes. Results show that it is obtained the lowest width of the ablation zone formed along the x axis is 14.58 mm, the highest width of the ablation zone formed along the x axis is 28.61 mm, the length of the ablation area obtained along the y axis was measured as 58.032 mm and about 5.44 cm^2 area of ablation zone. According to the temperature distance graph obtained along the vertical axis line in Figure 6.(b), it is observed that a minimum of 18,6 °C, maximum 100 °C in the regions seen in red and average 33,8 °C temperatures are reached. According to the temperature distance graph obtained along the vertical axis line in Figure 6.(d), it is seen that minimum 19.7 °C, maximum 101 °C in the regions seen in red and average 51.6 °C temperatures are reached. In terms of the obtained ablation zone diameter and the horizontal and vertical maximum lengths of the ablation zone, results close to the studies in the literature were obtained.

Contribution of Researchers

In the study carried out, Ahmet Rifat GÖRGÜN contributed in the titles of literature review, procurement of materials used, simulation, design and spelling. Adnan KAYA contributed to the formation of ideas, evaluation of the results obtained, and analysis of the results. Selçuk ÇÖMLEKÇİ, on the other hand, contributed to the control of the article in terms of content.

Conflict of Interest

There is no conflict of interest with any person/institution in the prepared article.

References

Ahmed, M., Brace, C.L., Lee, F.T.J., and Goldberg, S.N.(2011). Principles of and advances in percutaneous ablation, *Radiology,* 258(2), 351–369.

Ako, I.P. et al. (2019). A Study of the Radiation Characteristics of a Circular Loop Antenna Using Genetic Algorithm Technique, *International Journal of Applied Engineering Research*, 14(7), 1499-1504.

Amabile, C., Ahmed, M., Solbiati, L., Meloni, M.F., Solbiati, M., Cassarino, S., Tosoratti, N., Nissenbaum, Y., Ierace, T., Goldberg, S.N. (2017). Microwave ablation of primary and secondary liver tumours: ex vivo, in vivo, and clinical characterization, *International journal of hyperthermia,* Vol. 33, No. 1, 34–42.

Andreano, A., Huang, Y., Meloni, M.F., Lee, F.T., Brace, C. (2010). Microwaves create larger ablations than radiofrequency when controlled for power in ex vivo tissue, *Medical Physics,* 37(6), 2967– 2973.

Balanis, C.A. (1982). Antenna Theory: Analysis and Design, 2nd ed., Chapter 5, *John Wiley & Sons Inc.,* New York.

Bolton, T. (2016). Optimal Design of Electrically Small Loop Antenna Including Surrounding Medium Effects, *MSc Thesis, Georgia Institute of Technology*.

Brace, C.L. (2011). Dual-slot antennas for microwave tissue heating: Parametric design analysis and experimental validation, *Medical Physics,* 38(7), 4231–4240.

Brace, C.L. (2020). Microwave tissue ablation: biophysics,technology, and applications, *Critical* Reviews™ in *Biomedical Engineering*, 38, 65–78.

Brace, C.L., Laeseke, P.F., Van der Weide, P.D., and Lee, F.T. (2005). Microwave ablation with a triaxial antenna: Results in ex vivo bovine liver, *IEEE Transactions Microwave Theory Technology,* 53(1), 215–220.

Dielectric Properties of Body Tissues. (2021) Erişim adresi: http://niremf.ifac.cnr.it/tissprop/

Etoz, S. and Brace, C.L. (2018). Analysis of microwave ablation antenna optimization techniques, *International journal of RF Microwave Computer Aided Eng.,* 28:e21224.

Fadlallah, A.S., El-Bagoury, N., Gad, E.R.M.S., Ahmed, A.R., El-Ousamii, G. (2014). An Overview of NiTi shape memory alloy: Corrosion resistance and antibacterial inhibition for dental application, Journal of Alloys Compounds, 583, 455–464.

Fujimoto, K. and James, J.R. (2001). Mobile Antenna Systems Handbook, *2nd ed., Artech House.*

Ge, M., Jiang, H., Huang, X., Zhou, Y., Zhi, D., Zhao, G., Chen, Y., Wang, L., and Qiu, B. (2018). A multi-slot coaxial microwave antenna for liver tumor ablation, *Physics in Medicine and Biology,* 63, 1-13.

Goldberg, S.N., Gazelle, G.S., Dawson, S.L., Rittman, W., Mueller, P.R., Rosenthal, D.L. (1995). Tissue ablation with radiofrequenc : effect of probe size. gauge. duration. and temperature on lesion volume, *Acad Radio,* 2, 399-404.

Goldberg, S.N., Gazelle, G.S., Solbiati, L., Livraghi, T., Tanabe, K.K., Hahn, P.F., and Mueller, P.R. (1998). ‘Ablation of liver tumors using percutaneous RF therapy, *Ajr american journal of roentgenology,* vol. 170, no. 4, 1023–1028.

Görgün, A.R., Çömlekci, S., Kaya, A. (2019). Single Slot Coaxial Antenna and NiTi (Nickel Titanium) Loop Antenna Design for ISM (Industrial Scientific Medical) Band Microwave Ablation System, *Medical Technologies Congress (TIPTEKNO), IEEE 2019*.

Hamed, S.M.A. et al. (2014). Exact fields expressions for a circular loop antenna above a perfect electric conducting ground plane, *Sudan Engineering Society Journal*, 60(1).

Hancock, C.P. (2011). Electrosurgical apparatus for RF and microwave delivery, *U.S. Patent, 13/992,666.*

Hassan, E.G.M.I., Takruri, H., and Hope, M. (2016). Applicator design considerations of microwave tumor ablation, *In Proc. 10th International Symposium on Communication Systems , Networks and Digital Signal Processing*, 1–6.

Hodgson, D.A., Feldberg, I.B., Sharp, N., Cronin, N., Evans, M., and Hirschowitz, L. (1999). Microwave endometrial ablation: Development, clinical trials and outcomes at three years, *British Journal* of *Obstetrics* and *Gynaecology*, 106(7), 684–694.

Holton, A., Walsh, E., Anayiotos, A., Pohost, G., Venugopalan, R. (2002). Comparative MRI compatibility of 316 L stainless steel alloy and nickel titanium alloy stents, Original article technical, *Journal* of *Cardiovascular Magnetic Resonance,* 4(4), 423-430.

Hubner, F., Schreiner, R., Reimann, C., Bazrafshan, B., Kaltenbach, B., Schußler, M., Jakoby, R., and Vogl, T.J. (2019). Ex vivo validation of microwave thermal ablation simulation using different flow coefficients in the porcine liver, *Medical Engineering and Physics,* 66, 56-64.

Hurter, W., Reinbold, F., and Lorenz, W. (1991). A dipole antenna for interstitial microwave hyperthermia, *IEEE Transactions Microwave Theory Technology,* 39, 1048–1054.

Ibitoye, Z.A., Nwoye, E.O., Aweda, M.A., Oremosu, A.A., Annunobi, C.C., Akanmu, O.N. (2015). Optimization of dual slot antenna using floating metallic sleeve for microwave ablation, *Medical Engineering and Physics* 37, 384-391.

Kaur, S. and Maini, S. (2014). Microwave ablation therapy for the treatment of hepatocellular carcinoma using double slot interstitial antenna, *Internatıonal Journal Of Research In Computer Applıcatıons And Robotıcs*, 2(1), 56-61.

Lencioni, R., Goletti, O, Armillotta, N., Paolicchi, A., Moretti, M., Cioni, D., Donati, F., Cicorelli, A., Ricci, S., Carrai, M., Conte, P.F., Cavina, E., and Bartolozzi, C. (1998). Radio-frequency thermal ablation of liver metastases with a cooled-tip electrode needle: Results of a pilot clinical trial, *European Radiology,* vol. 8, no. 7, 1205–1211.

Liang ,P., Wang, Y. (2007). Microwave ablation of hepatocellular carcinoma, *Oncology,* 72 (1), 124–131.

Liu, E., Zong, Y., Chen, J., Zhang, X.J., Ren, R., Guo, X.C., Liu, Z.J., Lin, C.X. (2020). Cryoablation combined with radiotherapy for hepatic malignancy: Five case reports, *World Journal of Gastrointestinal Oncology,* 12(2), 237-247.

Liu, L.X., Zhang, W.H., Jiang, H.C. (2003). Current treatment for liver metastases from colorectal cancer, *World J Gastroenterol,* 9, 193-200.

Liu, W., Lin, X., Yang, F., Zeng, J., Song, H. and Cui, Y. (2016). Microwave Ablation Antenna with the ablation pattern being a figure-of-eight, *2016 IEEE MTT-S International Microwave Workshop Series on Advanced Materials and Processes for RF and THz Applications (IMWS-AMP),* 1-3.

Lubner, M.G., Brace, C.L., Hinshaw, J.L., Lee, F.T.J. (2010). Microwave tumor ablation: mechanism of action, clinical results and devices, *Journal of Vascular and Interventional Radiology,* 21, 192–203.

Luyen, H., Hagness, S.C. and Behdad, N. (2017). A Minimally Invasive Coax-Fed Microwave Ablation Antenna with a Tapered Balun*, IEEE Trans Antennas and Propagation*, 65(12).

Luyen, H., Hagness, S.C., and Behdad, N. (2015). A balun-free helical antenna for minimally-invasive microwave ablation, *IEEE Transactions Antennas Propagation,* 63(3), 959–965.

Mohtashami, Y., Hagness, S.C., and Behdad, N. (2017). A hybrid slot/monopole antenna with directional heating patterns for microwave ablation, *IEEE Transactions Antennas Propagation,* 65(8)8, 3889–3896.

Mohtashami, Y., Luyen, H., Sawicki, J.F., Shea, J.D., Behdad, N., and Hagness, S.C. (2018). Tools for attacking tumors: Performance comparison of triaxial, choke dipole, and balun-free base-fed monopole antennas for microwave ablation, *IEEE Antennas Propagation Magazine,* 60(6), 52–57.

Morgan, B.N. (2004). Medical shape memory alloy applications—The market and its products, *Materials Science and Engineering*, 378, 16–23.

Nan, Q., Zhang, H., Xia, Y., Oiao, A., Chang, Y., and Liu, Y. (2013). Thermal Field Analysis in Microwave Ablation Therapy for Atrial Fibrillation, *IEEE,* 585-588.

Niekerk, J.V. et al. (2002). Loop Antenna Basics and Regulatory Compliance for Short-Range Radio, *Microchip Technology Inc.*

O'Rourke, A.P., Haemmerich, D., Prakash, P., Converse, M.C., Mahvi, D.M., Webster, J.G. (2007). Current status of liver tumor ablation devices, *Expert Revision Medical Devices*, 4(4), 523-37.

Phasukkit, P., Wongketsada, T. (2021). Triple coaxial-half-slot antenna scheme with deep learning-based temperature prediction for hepatic microwave ablation: Finite element analysis and in Vitro experiment, *IEEE Engineering in Medicine and Biology Section.*

Prakash, P. (2010). Theoretical modeling for hepatic microwave ablation, *Open Biomedical Engineering Journal,* 4, 27–38.

Reimann, C.H.N., Bazrafshan, B., Schußler, M., Schmidt, S., Schuster, C., Hubner, F., Vogl, T.J., and Jakoby, R. (2019). A dual mode coaxial slot applicator for microwave ablation treatment, *IEEE Transactions on Microwave Theory and Techniques,* 67, 1255-1264.

Seifert, J., Junginger, T., and Morris, D. (1998). A collective review of the world literature on hepatic cryotherapy, *Journal of the Royal College of Surgeons of Edinburgh,* 43(3), 141–154.

Seki, T., Wakabayashi, M., Nakagawa, T., Itoh, T., Shiro, T., Kunieda, K., Sato, M., Uchiyama, S. and Inoue, K. (1994). Ultrasonically guided percutaneous microwave coagulation therapy for small hepatocellular carcinoma, *Liver Cancer,* 74, 814–825.

Shock, S.A., Meredith, K., Warner, T.F., Sampson, L.A., Wright, A.S., Winter, T.C., Mahvi, D.M., Fine, J.P., and Lee, F.T. (2004). 'Microwave ablation with loop antenna: In vivo porcine liver model, *Radiology,* 231(1), 143–149.

Song, C. (2010). History and current situation of shape memory alloys devices for minimally invasive surgery, *Open Medical Devices Jornal*, 2, 24-31.

Sugiyama, M., Saito, K. (2018). Article Characteristics of a Surgical Snare Using Microwave Energy, *Diagnostics*, 8, 83, 2018.

Tamilarasan, A.K., Krishnadhas, S.K., Sabapathy, S., Sarasa, A.S.T. (2021). A novel design of Rogers RT/duroid 5880 material based two turn antenna for intracranial pressure monitoring, *Microsystem Technologies*, 27, 3579–3588.

Torre, L.A., Siegel, R.L., Ward, E.M., Jemal, A. (2016). Global cancer incidence and mortality rates and trends—an update, *Cancer Epidemiol Biomarkers Prevention,* 25, 16–27.

Wright, A.S., Lee, F.T., Mahvi, D.M. (2003). Hepatic microwave ablation with multiple antenna results in synergistically larger zones of coagulation necrosis, Annals of *Surgical Oncology,* 10,275-283.

Wright, A.S., Sampson, L.A., Warner, T.F., et al. (2005). Radiofrequency versus microwave ablation in a hepatic porcine model, *Radiology,* 236, 132–139.

Yang, D. et al. (2006). A floating sleeve antenna yields localized hepatic microwave ablation, *IEEE Transactions on Biomedical Engineering,* 53(3), 533-537.

Yang, D.S., Converse, M.C., Mahvi D.M., and Webster, J.G. (2007). Expanding the bioheat equation to include tissue internal water evaporation during heating, *IEEE Transactions Biomedical Engineering,* 54(8),1382–1388.